

Supplementary data

1. **Table S1.** Purification of wild-type and mutant 3 $\alpha$ -HSD/CRs

2. **Table S2.** The T<sub>m</sub> values and protein tryptophan intrinsic fluorescence of wild-type and mutant 3 $\alpha$ -HSD/CRs.

3. **Table S3.** Oligonucleotide primers used for site-directed mutagenesis.

4. **Figure S1. The SDS-PAGE analysis of mutant 3 $\alpha$ -HSD/CR expressed in *E. coli* BL21(DE3).** The expression and purification of I13K mutant. The molecular mass marker (kDa; M). Lanes 1 and 2, total proteins of BL21 containing I13K mutant in the absence and presence of IPTG induction, respectively. Lane 3 and 4, supernatant and pellet after cell lysis by sonication. Lanes 5, elution fractions from His-bind Ni-NTA affinity column in absence of imidazole. Lanes 6-12, elution fractions from His-bind Ni-NTA affinity column in presence of 0, 50, 50, 100, 200, 300, and 300 mM imidazole, respectively. Fractions of lanes 10-12 are collected for dialysis.

5. **Figure S2. Molecular docking analysis of NAD<sup>+</sup> and NMN<sup>+</sup> for wild-type and mutant 3 $\alpha$ -HSD/CRs.** The NAD<sup>+</sup> bound binary complex of wild-type 3 $\alpha$ -HSD/CR is from the crystal structure (pdb:1fk8). The three-dimensional diagrams display the docking result for the interaction of wild-type and mutants of T11A, T11K, T11R, I13A, I13K, I13R, D41I, D41Q, A70I, A70K, A70Q, I112A, and I112K 3 $\alpha$ -HSD/CRs with NAD<sup>+</sup> or NMN<sup>+</sup>, respectively. The two-dimensional diagrams show the interactions of the amino acid residues in the binding pocket of enzymes to NAD<sup>+</sup> or NMN<sup>+</sup>. The types of interactions are indicated by the colors of residues indicate and bond distances ( $\text{\AA}$ ) are shown on each interaction.

**Table S1. Purification of wild-type and mutant 3 $\alpha$ -HSD/CRs<sup>a</sup>.**

Enzyme	WT	T11A	T11K	T11R	I13A	I13K	I13K <sup>b</sup>	I13R	I13R <sup>b</sup>	D41I	D41Q	D41Q <sup>b</sup>	A70I	A70I <sup>b</sup>	A70Q	A70K <sup>b</sup>	I112A	I112K
Wet pellet (g)	2.4	3.0	3.8	2.6	3.2	2.7	2.5	3.6	3.6	1.9	2.7	3.6	3.3	3.8	1.7	3.6	2.9	2.4
Yield (mg)	38.8	6.7	11.4	10.3	13.8	4.1	25.9	2.4	35.6	4.3	1.7	10.0	0.9	26.7	17.7	59.1	13.9	7.3
Inclusion body <sup>c</sup>	-	-	-	-	-	+	-	+	-	+	+	+	+	+	-	-	-	-

<sup>a</sup>3 $\alpha$ -HSD/CRs are overexpressed in *E. coli* BL21 in 1 liters LB medium, induced by 0.5 mM IPTG at 37 °C and purified by metal-chelate chromatography. <sup>b</sup> Protein expression induced by IPTG at lower temperatures 14 °C for 14 hrs. <sup>c</sup> -, no inclusion body observed; +, Inclusion body formed.

**Table S2. The T<sub>m</sub> values and protein tryptophan intrinsic fluorescence of wild-type and mutant 3 $\alpha$ -HSD/CRs<sup>a,b</sup>.**

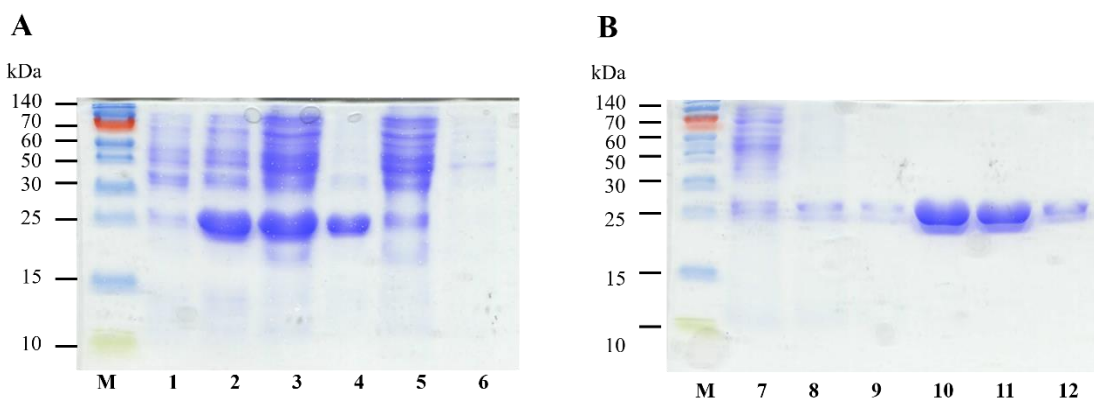
3 $\alpha$ -HSD/CR	WT	T11A		T11K		T11R		I13A		I13K		I13R		D41I		D41Q		A70I		A70Q		A70K		I112A		I112K		
		T <sub>m1</sub>	T <sub>m2</sub>																									
T <sub>m</sub>	51.9	32.2	50.5	30.5	48.5	32.0	49.1	32.8	45.8	32.0	41.3	35.4	48.3	46.8	29.4	41.4	50.8	46.6	51.4	51.6	60.4							
$\lambda_{\text{max}}$	329	329	329		331		329		329		330	336	335		332		329	329	329	329	329	329						
F <sub>max</sub>	529	521	518		506		473		477		522	350	442		492		523	495	546	549								

<sup>a</sup> The T<sub>m</sub> values of wild-type and mutant 3 $\alpha$ -HSD/CRs are obtained from the thermal unfolding by DSF. T<sub>m1</sub> and T<sub>m2</sub> are the midpoint temperatures for the thermal unfolding transition from a native state to an intermediate state and an intermediate state to an unfolded state, respectively. <sup>b</sup> The protein fluorescence spectra of 4  $\mu$ M wild-type and mutant 3 $\alpha$ -HSD/CRs excited at 295 nm, pH 7.5.  $\lambda_{\text{max}}$  and F<sub>max</sub> are the maximum wavelength and intensity, respectively.

**Table S3. Oligonucleotide primers used for site-directed mutagenesis**

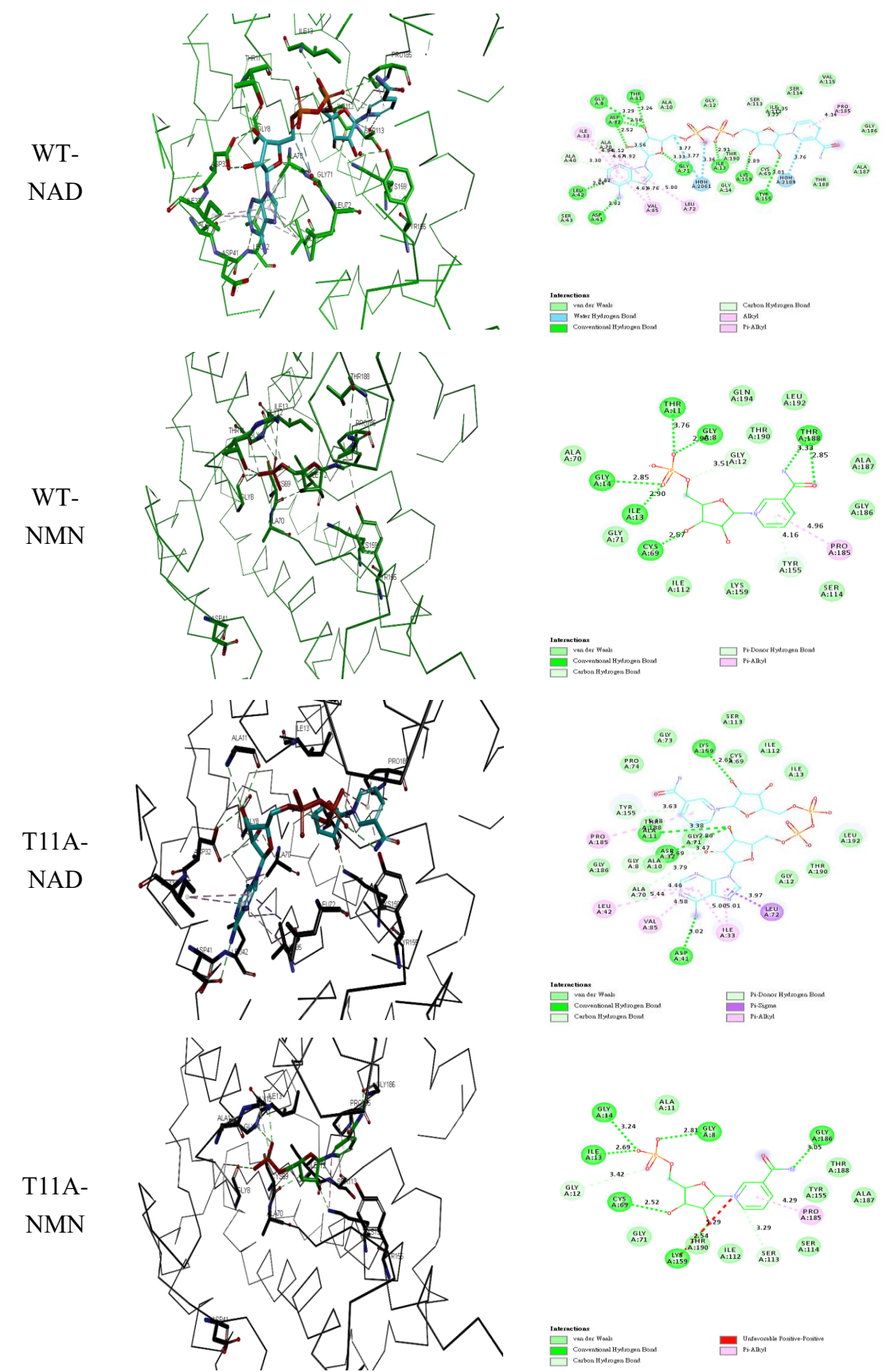
Mutation	Direction	Nucleotide sequence of primer <sup>a</sup>
T11A	Forward	5'-gcggctgcgcc <u><b>g</b></u> ccggatttgtcg-3'
	Reverse	5'-cgcaccaatgcc <u><b>gg</b></u> ccggcagccgc-3'
T11R	Forward	5'-gcggctgcgcc <u><b>a</b></u> ggggatttgtcg-3'
	Reverse	5'-cgcaccaatgcc <u><b>c</b></u> ttggcgcagccgc-3'
T11K	Forward	5'-gcggctgcgcc <u><b>a</b></u> aggcatttgtcg-3'
	Reverse	5'-cgcaccaatgcc <u><b>c</b></u> ttggcgcagccgc-3'
I13A	Forward	5'-ctgcgccaccggc <u><b>g</b></u> cttgtcggtacg-3'
	Reverse	5'-cgtagccgcacc <u><b>a</b></u> gggtggcgtacg-3'
I13R	Forward	5'-ctgcgccaccggc <u><b>a</b></u> gggttgtcggtacg-3'
	Reverse	5'-cgtagccgcacc <u><b>c</b></u> tttgtcggtacg-3'
I13K	Forward	5'-ctgcgccaccggc <u><b>a</b></u> gggttgtcggtacg-3'
	Reverse	5'-cgtagccgcacc <u><b>c</b></u> tttgtcggtacg-3'
D41Q	Forward	5'-gaagtgattgcc <u><b>c</b></u> agctctcgacggccg-3'
	Reverse	5'-cggccgtcgag <u><b>a</b></u> ctggcaatcacttc-3'
D41I	Forward	5'-gaagtgattgcc <u><b>a</b></u> ttctctcgacggccg-3'
	Reverse	5'-cggccgtcgag <u><b>a</b></u> atggcaatcacttc-3'
A70I	Forward	5'-ctggtgtgtgc <u><b>a</b></u> tggcctggaccg-3'
	Reverse	5'-cggtcccagggcc <u><b>a</b></u> tgcacagcaccag-3'
A70Q	Forward	5'-ctggtgtgtgc <u><b>c</b></u> aggcctggaccg-3'
	Reverse	5'-cggtcccagggcc <u><b>c</b></u> ttgcacagcaccag-3'
A70K	Forward	5'-ctggtgtgtgc <u><b>a</b></u> aggcctggaccg-3'
	Reverse	5'-cggtcccagggcc <u><b>c</b></u> ttgcacagcaccag-3'
I112A	Forward	5'-gcagccgtgtc <u><b>g</b></u> ccctgtccgtggcttc-3'
	Reverse	5'-gaagccacggac <u><b>g</b></u> gacgacggctgc-3'
I112K	Forward	5'-gcagccgtgtc <u><b>a</b></u> gtgtccgtggcttc-3'
	Reverse	5'-gaagccacggac <u><b>a</b></u> ttgtacgacggctgc-3'

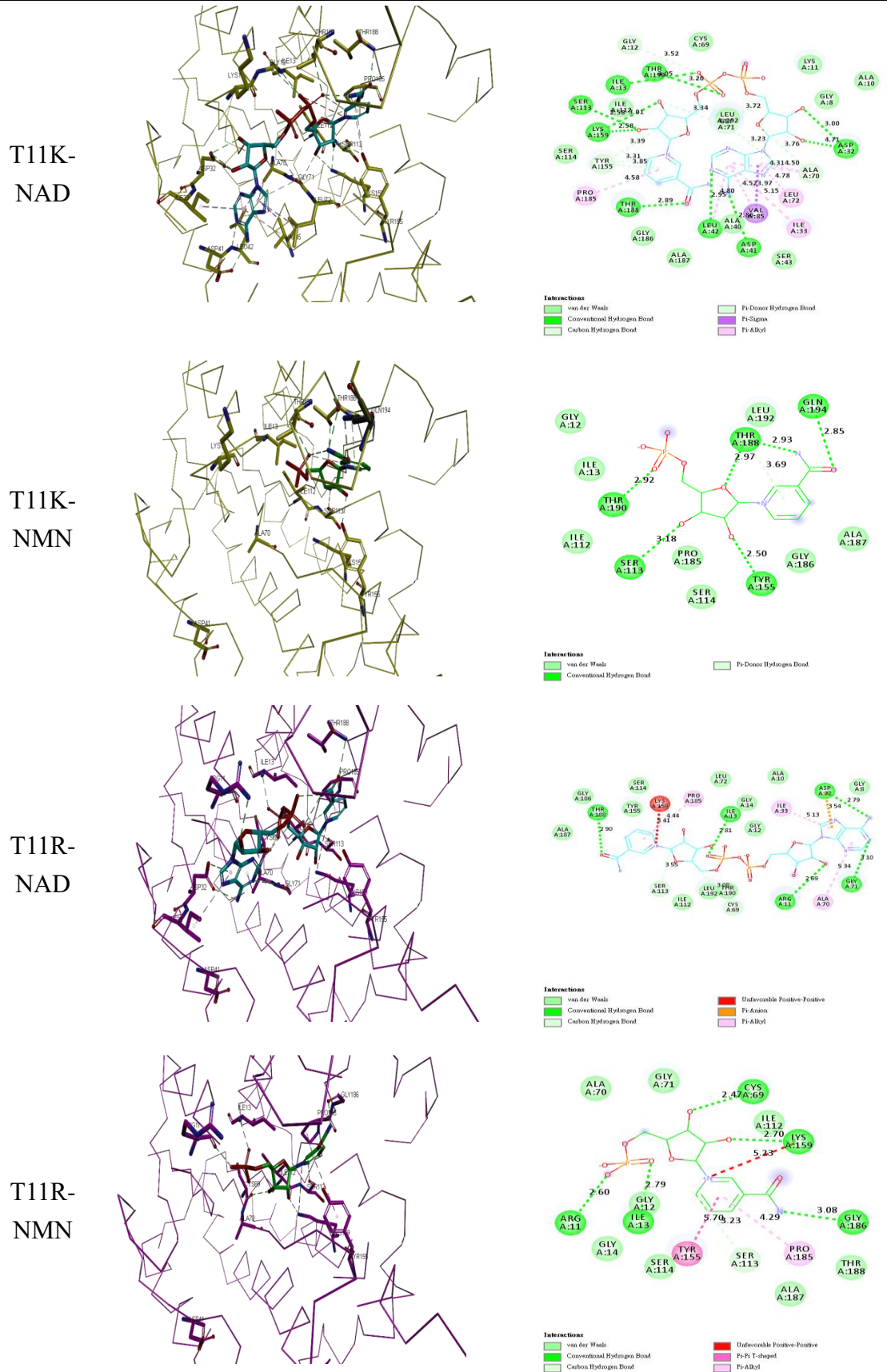
<sup>a</sup>The boldface codons indicate the mutation on the amino acid residues and the underlined codons indicate the site of the mutation.

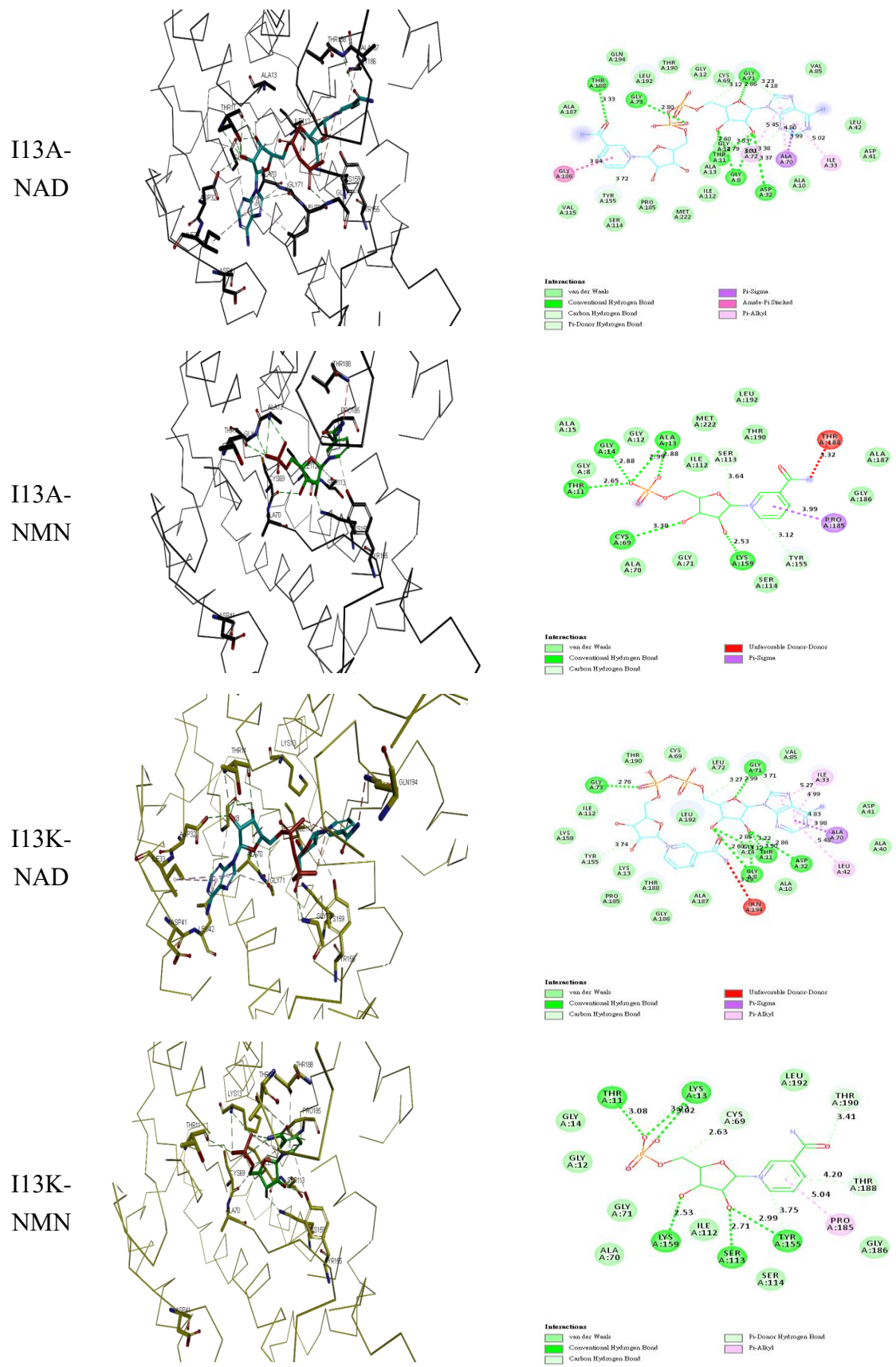


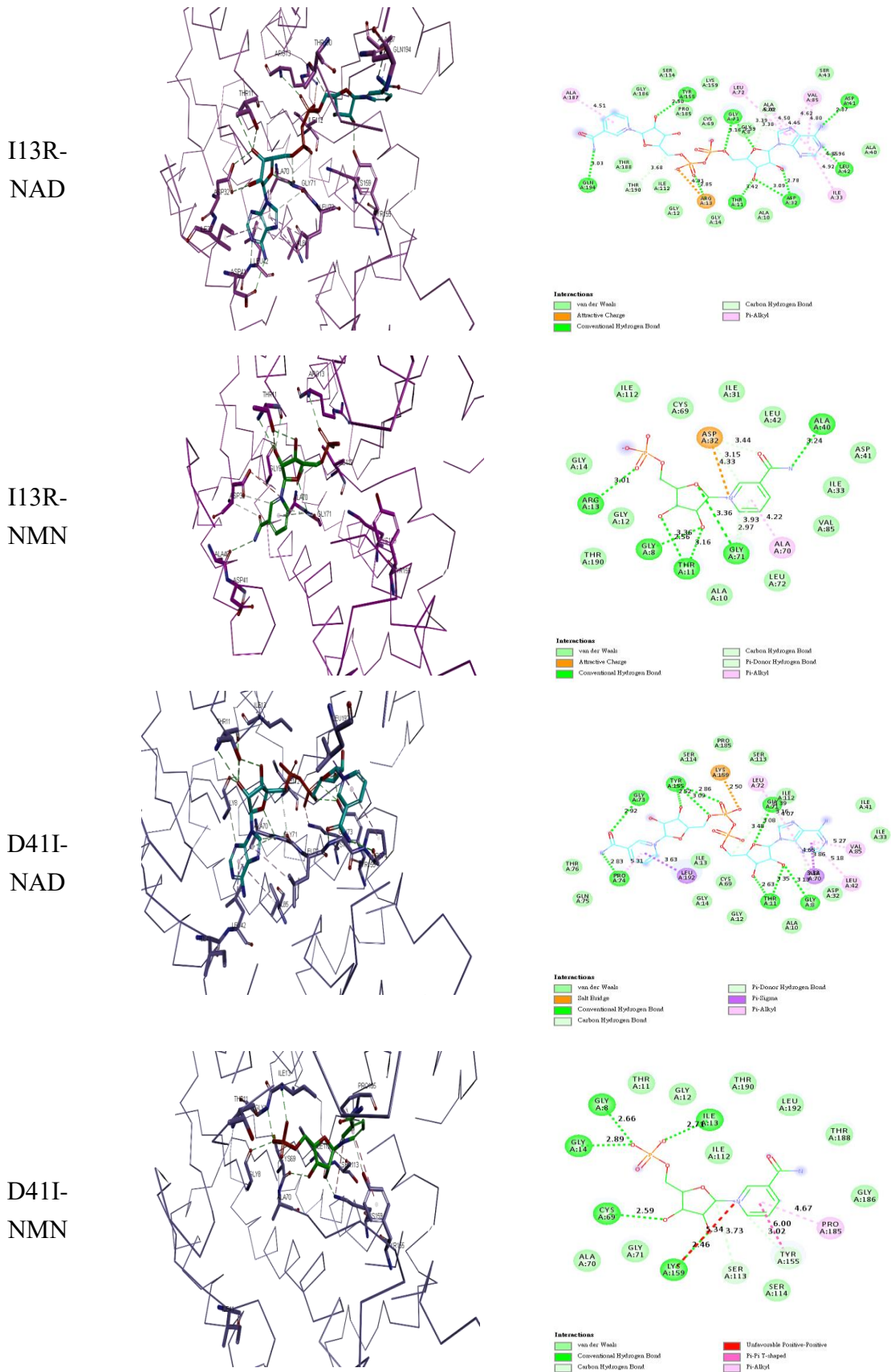
**Figure S1. The SDS-PAGE analysis of mutant 3 $\alpha$ -HSD/CR expressed in *E. coli* BL21(DE3).** The expression and purification of I13K mutant. The molecular mass marker (kDa; M). Lanes 1 and 2, total proteins of BL21 containing I13K mutant in the absence and presence of IPTG induction, respectively. Lane 3 and 4, supernatant and pellet after cell lysis by sonication. Lanes 5, elution fractions from His-bind Ni-NTA affinity column in absence of imidazole. Lanes 6-12, elution fractions from His-bind Ni-NTA affinity column in presence of 0, 50, 50, 100, 200, 300, and 300 mM imidazole, respectively. Fractions of lanes 10-12 are collected for dialysis.

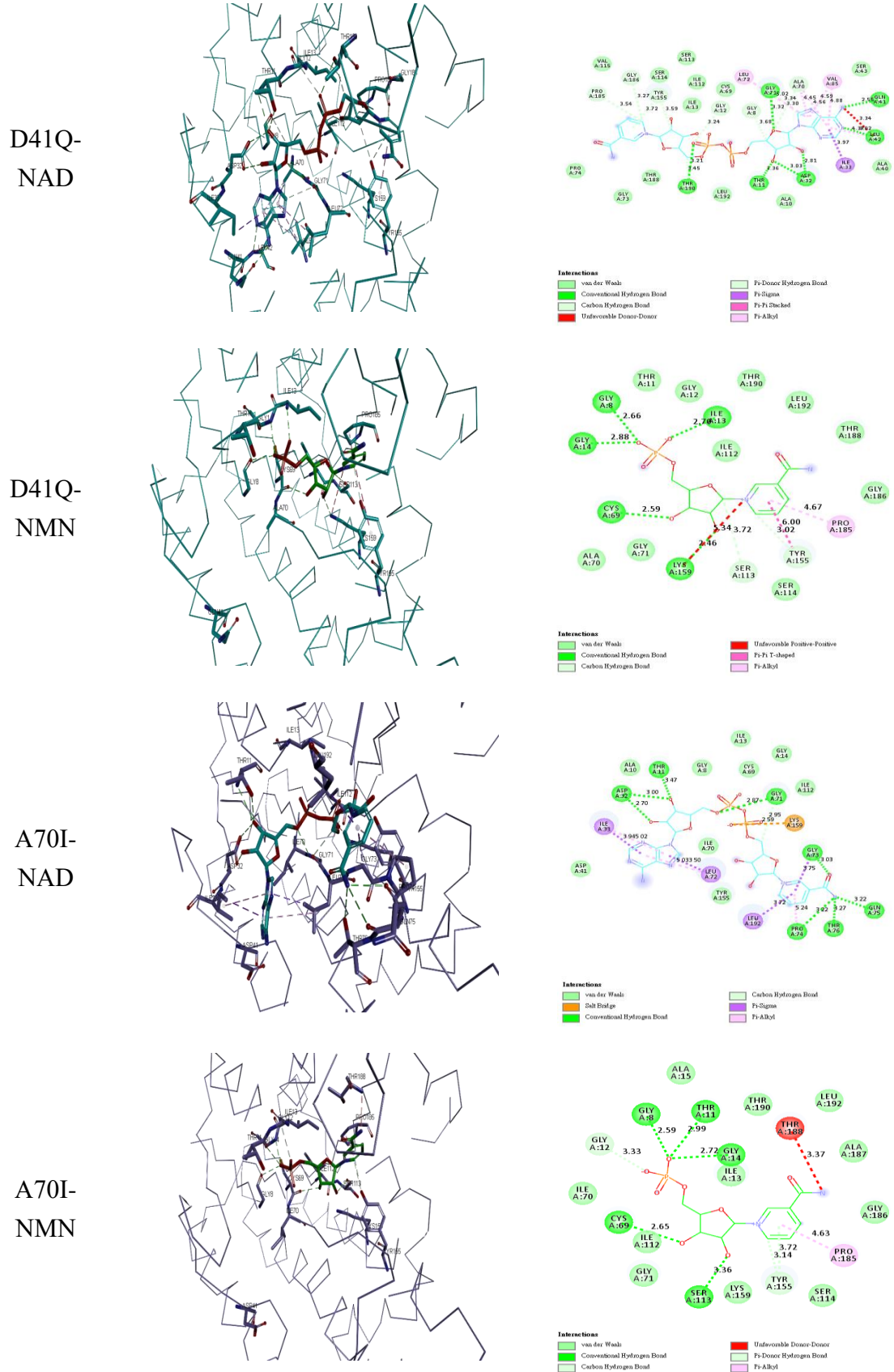
**Figure S2.**

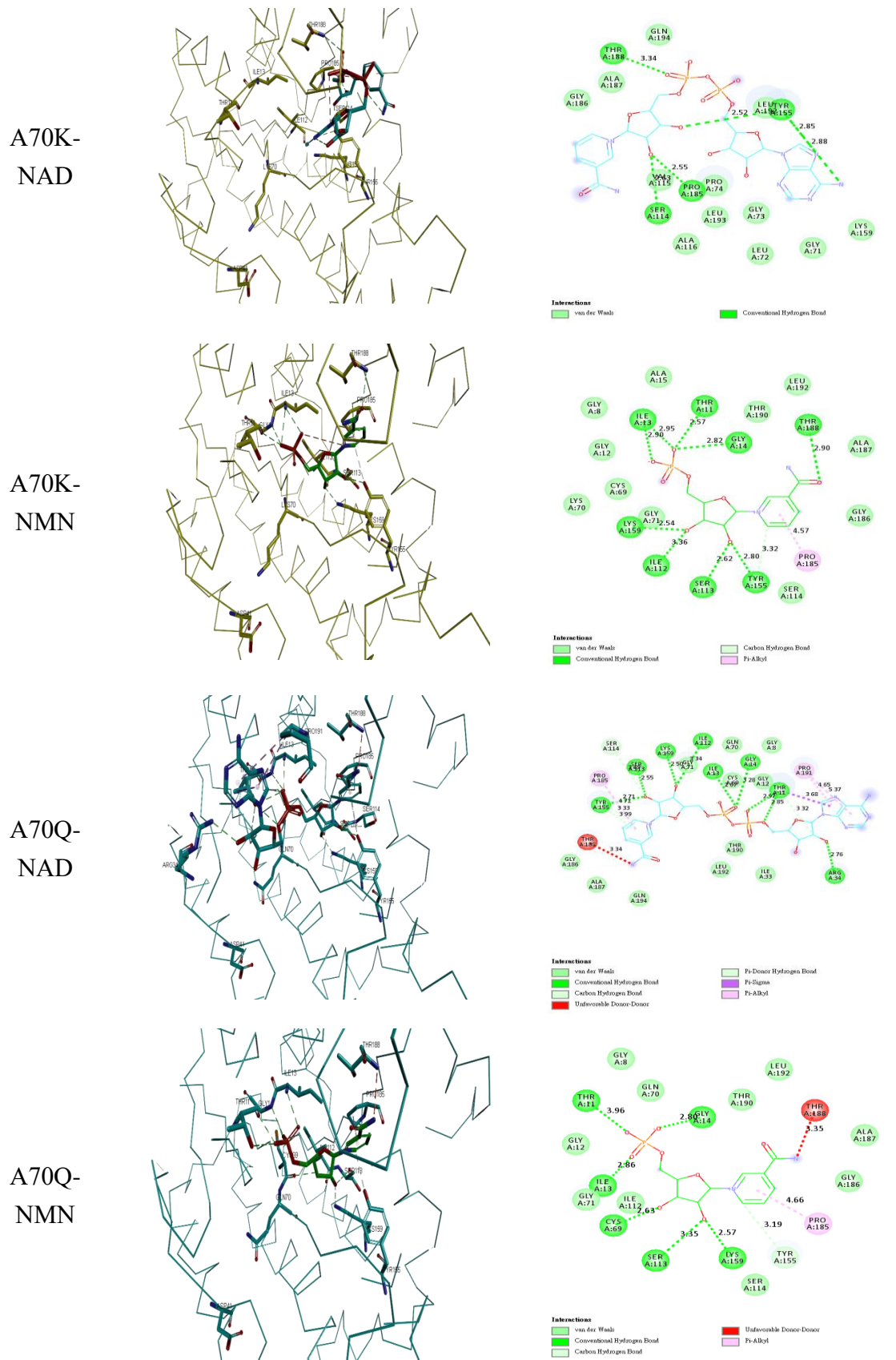


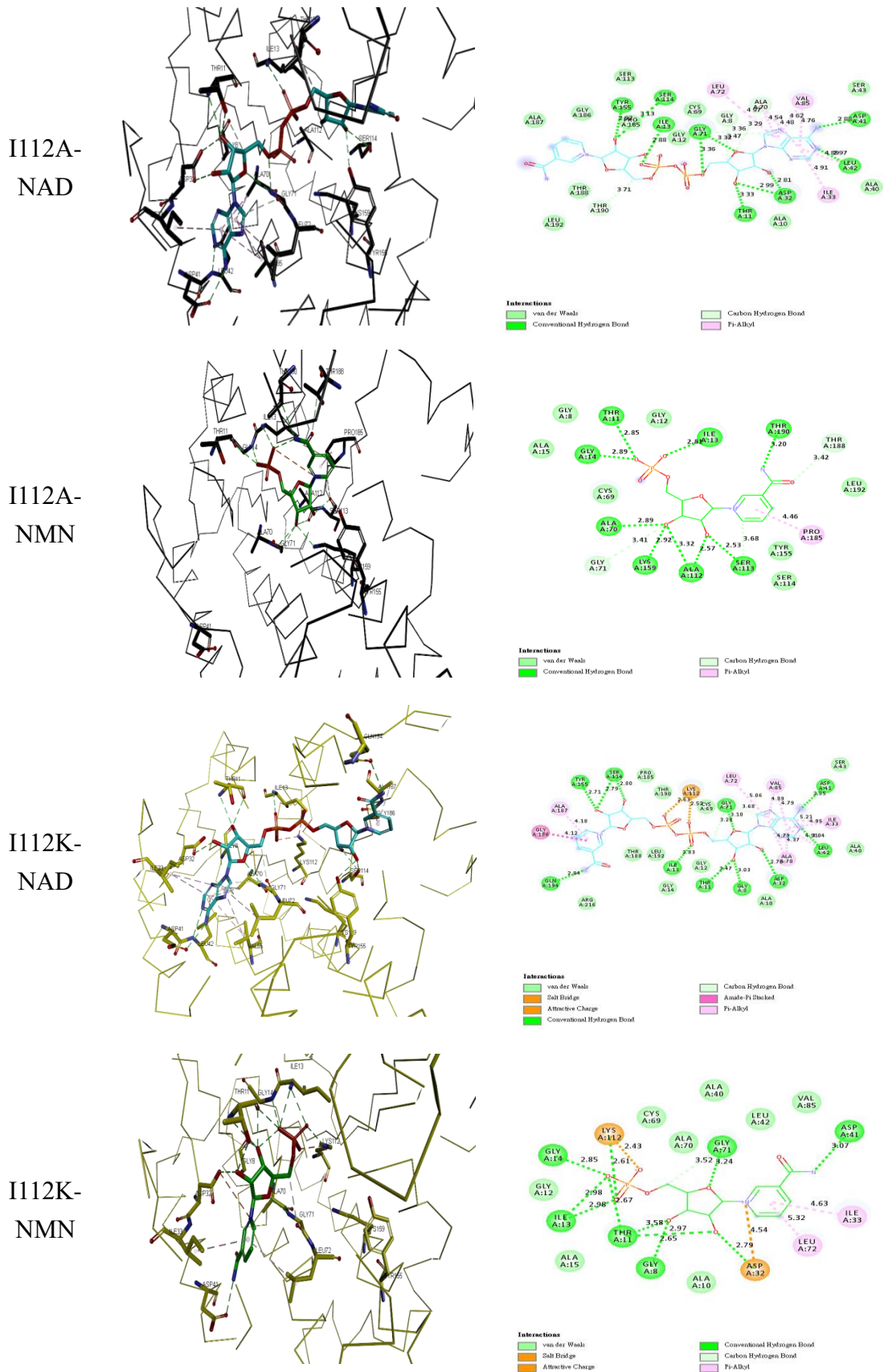












**Figure S2. Molecular docking analysis of NAD<sup>+</sup> and NMN<sup>+</sup> for wild-type and mutant 3 $\alpha$ -HSD/CRs.** The NAD<sup>+</sup> bound binary complex of wild-type 3 $\alpha$ -HSD/CR is from the crystal structure (pdb:1fk8). The three-dimensional diagrams display the docking result for the interaction of wild-type and mutants of T11A, T11K, T11R, I13A, I13K, I13R, D41I, D41Q, A70I, A70K, A70Q, I112A, and I112K 3 $\alpha$ -HSD/CRs with NAD<sup>+</sup> or NMN<sup>+</sup>, respectively. The two-dimensional diagrams show the interactions of the amino acid residues in the binding pocket of enzymes to NAD<sup>+</sup> or NMN<sup>+</sup>. The types of interactions are indicated by the colors of residues indicate and bond distances ( $\text{\AA}$ ) are shown on each interaction.